MPMI Vol. 37, No. 2, 2024, pp. 98–111, https://doi.org/10.1094/MPMI-04-23-0045-R

Interaction of Whitefly Effector G4 with Tomato Proteins Impacts Whitefly Performance

Diana Naalden,[1,2] Wannes Dermauw,[3,4] Aris Ilias,[5] Geert Baggerman,[6,7] Marieke Mastop,[2] Juliette J. M. Silven,[2] Paula J. M. van Kleeff,[2] Sarmina Dangol,[2] Nicolas Frédéric Gaertner,[2] Winfried Roseboom,[8] Mark Kwaaitaal,[2] Gertjan Kramer,[8] Harrold A. van den Burg,[2] John Vontas,[5,9] Thomas Van Leeuwen,[3] Merijn R. Kant,[1] and Robert C. Schuurink[2,†]

[1] Department of Evolutionary and Population Biology, Institute for Biodiversity and Ecosystem Dynamics, University of Amsterdam, 1098 XH Amsterdam, The Netherlands
[2] Green Life Sciences Research Cluster, Swammerdam Institute for Life Sciences, University of Amsterdam, 1098 XH Amsterdam, The Netherlands
[3] Department of Plants and Crops, Faculty of Bioscience Engineering, Ghent University, 9000 Ghent, Belgium
[4] Flanders Research Institute for Agriculture, Fisheries and Food, Plant Sciences Unit, 9820 Merelbeke, Belgium
[5] Institute of Molecular Biology & Biotechnology, Foundation for Research & Technology Hellas, 70013 Heraklion, Crete, Greece
[6] Centre for Proteomics, University of Antwerp, 2020 Antwerp, Belgium
[7] Unit Environmental Risk and Health, Flemish Institute for Technological Research, 2400 Mol, Belgium
[8] Laboratory for Mass Spectrometry of Biomolecules, University of Amsterdam, 1098 XH Amsterdam, The Netherlands
[9] Laboratory of Pesticide Science, Department of Crop Science, Agricultural University of Athens, Athens, Greece

Accepted for publication 28 November 2023.

The phloem-feeding insect *Bemisia tabaci* is an important pest, responsible for the transmission of several crop-threatening virus species. While feeding, the insect secretes a cocktail of effectors to modulate plant defense responses. Here, we present a set of proteins identified in an artificial diet on which *B. tabaci* was salivating. We subsequently studied whether these candidate effectors can play a role in plant immune suppression. Effector G4 was the most robust suppressor of an induced- reactive oxygen species (ROS) response in *Nicotiana benthamiana*. In addition, G4 was able to suppress ROS production in *Solanum lycopersicum* (tomato) and *Capsicum annuum* (pepper). G4 localized predominantly in the endoplasmic reticulum in *N. benthamiana* leaves and colocalized with two identified target proteins in tomato: REF-like stress related protein 1 (RSP1) and meloidogyne-induced giant cell protein DB141 (MIPDB141). Silencing of *MIPDB141* in tomato reduced whitefly fecundity up to 40%, demonstrating that the protein is involved in susceptibility to *B. tabaci*. Together, our data demonstrate that effector G4 impairs tomato immunity to whiteflies by interfering with ROS production and via an interaction with tomato susceptibility protein MIPDB141.

Keywords: insect resistance, plant defense, plant immune suppression, VIGS, whiteflies

[†]Corresponding author: R. C. Schuurink; R.C.Schuurink@uva.nl

Author contributions: D.N., R.C.S., M.R.K., T.V.L., and J.V. conceived the experiments. D.N. performed the cloning procedures, ROS assays, VIGS, and bioassays. M.M. and P.J.M.v.K. performed confocal microscopy. A.I. collected artificial diet with whitefly saliva. G.B. performed LC-MS/MS experiments. and W.D. analyzed artificial diet LC-MS/MS data. J.J.M.S. performed qPCR. S.D. performed phloem extraction. G.K. and W.R. performed LC-MS/MS experiments and analyzed LC-MS/MS data of phloem exudate. N.F.G. and M.R.K. performed the vector adaptation for split-luciferase and wrote the materials and methods for this part. H.A.v.d.B. supervised N.F.G. and M.R.K. D.N., W.D., M.R.K., and R.C.S. wrote the manuscript. All authors have read and agreed on the content.

Funding: This research is funded by the European Union's Horizon 2020 research and innovation program (773 902-SuperPests) and by the Dutch Research Council (NWO) grant 19391 (TTI-VICI). S. Dangol was supported under the European Union's Horizon 2020 research and innovation program (817526–PRE-HLB). P. J. M. van Kleeff and M. Mastop were supported by NWO-TTW grant 16319. The Topsector T&U program (https://topsectortu.nl) Better Plants for Demands (grant 1409-036 to H. A. van den Burg), including the partnering breeding companies, supported the work on the vector optimalization related to the luciferase complementation assay.

e-Xtra: Supplementary material is available online.

The author(s) declare no conflict of interest.

The silverleaf whitefly, *Bemisia tabaci*, is a priority pest globally. It has a broad host range and the direct and indirect damage it inflicts causes tremendous economic losses in agriculture (Saurabh et al. 2021). Direct damage is caused by the insect's phloem feeding, while the major indirect damage is a result of the transmission of many plant-damaging viruses (reviewed in Fiallo-Olivé et al. 2020) and secretion of honeydew that attracts secondary plant-damaging organisms. *B. tabaci* comprises a species complex of more than 40 cryptic species with, for example, variation in host range, insecticide resistance, virus transmission, morphometrics, and genetics (De Barro et al. 2011; Mugerwa et al. 2018, 2021). Within this species complex, Mediterranean (MED, also known as the Q biotype) and Middle-East-Asia Minor 1 (MEAM1, also known as the B biotype or *Bemisia argentifolii*) are among the best studied (Boykin et al. 2013).

Whiteflies are herbivores that live in close contact with their host and depend on them throughout their life cycle. The insect

uses its stylet to penetrate the leaf tissue via the apoplast to feed from the contents of the phloem. Eggs are deposited on the abaxial side of the leaf and hatch after 5 to 9 days, from which the mobile juveniles (crawlers) emerge. The crawlers start searching for a suitable feeding site and then molt into sessile nymphs. The immobile nymphs use a single feeding site where they develop over several weeks (depending on environmental conditions) through four nymphal stages into adults (Gangwar and Gangwar 2018).

Whitefly feeding is rapidly detected by plants, triggering the plant's immune response. During this interaction, the plant can execute a set of physiological changes to defend itself. These include the induction of several phytohormone-mediated defense pathways, of which the jasmonate (JA) signaling pathway is the most important. Other strategies include the induction of the production of specialized metabolites, such as terpenoids, glucosinolates, or phenolic compounds (reviewed in Li et al. 2023) and increasing the cuticle thickness (Firdaus et al. 2011). Plants recognize conserved herbivore-associated molecular patterns as well as damage-associated molecular patterns (DAMPs) caused by feeding, which induces production of reactive oxygen species (ROS) (Snoeck et al. 2022). This also connects to the fact that several whitefly effectors have been shown to reduce ROS accumulation in planta (Su et al. 2019; Wang et al. 2019).

These defense responses are often insufficient to reduce damage to levels acceptable for crops (Naalden et al. 2021). Pesticides are frequently used to control whiteflies, but their use can have undesirable impacts on the environment and on human health. In addition, frequent use of pesticides against *B. tabaci* often results in a quick selection for resistance (Horowitz et al. 2020; Patra and Kumar Hath 2022). Biocontrol, for example, by means of entomopathogenic fungi or parasitoids, can be effective, yet its applicability is limited across different environmental conditions and takes a relatively long time (Liu et al. 2015; Sani et al. 2020). Therefore, generating whitefly-resistant plant varieties is an important strategy for disease management. To date, only one resistance gene, *Mi-1.2*, provides enhanced resistance against both MED and MEAM1 biotypes in tomato (*Solanum lycopersicum*). However, *Mi-1.2* does not provide resistance at higher temperatures or in younger tomato plants (Nombela et al. 2003) and thus has limited applicability.

Research has shown that salivary proteins (effectors) secreted during feeding dampen the induced defense response to levels the whitefly can cope with (Naalden et al. 2021). Some of these immune-suppressing effectors have been identified and characterized for *B. tabaci*. For example, the ferritin effector BtFer1 suppresses ROS production, callose deposition, and JA-mediated signaling pathways (Su et al. 2019). For effectors Bsp9 and Bt56, proteinaceous targets were identified in planta and were shown to be involved in plant immunity (Wang et al. 2019; Xu et al. 2019)). Furthermore, effectors 2G4, 2G5, and 6A10 suppress the disease symptoms induced by *Ralstonia solanacearum* (Lee et al. 2018). Two other whitefly effectors, BtArmet and BtE3, have been characterized. BtArmet interacts with a cystatin, NtCYS6, to overcome the negative effect of plant defense on whitefly performance (Du et al. 2022). BtE3 is able to inhibit the *Burkholderia glumae*-induced hypersensitive response (HR) in *Nicotiana benthamiana* and tomato (Peng et al. 2023).

For successful resistance breeding, one can start with modifying effector targets that act as susceptibility factors (Tyagi et al. 2020). However, as whiteflies can adapt, a comprehensive overview of effector diversity and, subsequently, effector targets is much desired. In this study, we identified a set of candidate effectors that were present in the saliva of *B. tabaci* (MED) and characterized one of these, named G4, for its in planta targets and its effect on plant immunity.

Results

At least seven candidate effectors could be identified in an artificial diet

To identify candidate effectors, adult whiteflies (MED) were fed with an artificial diet that was analyzed for the presence of proteins (Supplementary Table S1). Two *B. tabaci* proteins/protein groups, BTA026858.1 (S2; van Kleeff et al. 2023) and BTA009432.1 (S1; van Kleeff et al. 2023)/BTA009433.1, were identified in artificial diet collected after 6 h of *B. tabaci* feeding. In artificial diet collected after 24 h of *B. tabaci* feeding, nine proteins/protein groups were identified BTA026858.1 (S2), BTA009432.1 (S1)/BTA009433.1 together with BTA002396.1 (G1-d), BTA023203.2 (G2), BTA007921.1 (G3; named BtE3 by Peng et al. 2023), BTA018678.1, BTA003195.1/BTA027670.1, BTA007014.1/BTA027040.1, and BTA021638.1 (G4) (Supplementary Table S2). For all samples, the highest number of peptides was found for BTA026858.1 (S2), and to a lesser extent for BTA009432.1 (S1). Based on a tblastn search, eight of the nine identified proteins (or protein groups) have been previously identified in *B. tabaci* (MED) artificial diet by Huang et al. (2021) (Supplementary Table S3). Based on another study, the genes encoding S1, S2, and BTA023203.2 (G2) are the three most highly expressed genes in *B. tabaci* MED heads, while the other identified proteins are encoded by genes belonging to the top 2% of most highly expressed genes in *B. tabaci* MED heads (Wang et al. 2020; Supplementary Table S3). Seven of the nine identified proteins/protein groups were predicted to include a signal peptide (Supplementary Table S2). We continued with a subset of these proteins for further characterization using the following criteria: two proteins (groups) were excluded in further functional analysis, as they were characterized in another project (S1 and S2), and further selection was made based on the presence of a signal peptide, which led to the selection of four interesting candidate effector proteins (G1 to G4). *G1* was found to have a potential paralog (*G1-t*) in the *B. tabaci* MEAM1 transcriptome (Lee et al. 2018; van Kleeff et al. 2023), and therefore both were further analyzed for their role in immune suppression. Sequence information can be found in Supplementary Figure S1.

G4 suppresses flg22-induced ROS in several plant species

To investigate whether the selected candidate effectors were able to modulate the early immune response of the plant, we performed ROS assays in *N. benthamiana.* Effectors were transiently expressed in planta, and leaf tissue was subsequently exposed to the pattern-associated molecular pattern (PAMP) peptide flg22 to induce ROS production. Expression of *G1* resulted in a mixed response in the ROS assays: in some cases, significantly less H_2O_2 was measured compared with free cyan fluorescent protein (CFP) as negative control (Fig. 1); and in other cases, the H_2O_2 level was lower, albeit not statistically significant. This was the case for both G1 retrieved from the artificial diet (G1-d) and the G1 paralog retrieved from the transcriptomic data (G1-t). Expression of *G2* or *G3* did not result in significant reduction of ROS production.

Effector G4 suppressed the flg22-induced ROS significantly compared with the CFP control (Fig. 2) in *N. benthamiana* and was the most robust suppressor of the four candidate effectors selected from the artificial diet. To test whether this effector also affects immune responses of other plant species, we performed the flg22-induced ROS assay using leaf disks of the crop plants *S. lycopersicum* and *Capsicum annuum* (pepper) transiently expressing *G4* (Fig. 2). In both these plant species, G4 reduced the ROS production, but not as efficiently as observed in *N. benthamiana*. In the early stage (first 18 min), G4 significantly reduced the ROS production in *S. lycopersicum* compared with CFP. The effector also caused a delay in the peak of the burst,

but the total production of ROS after 45 min was almost similar to that of the CFP control. In addition, G4 suppressed ROS in *C. annuum* in the first 23 min, but the final ROS production was not significantly different after 45 min either. A representation of the ROS production for each time point can be found in Supplementary Figure S3.

G4 encodes a protein with a predicted size of 267 amino acids and is whitefly specific

To obtain more insight into whether *G4* is present in *B. tabaci* MEAM1 and may be part of a gene family, we performed a BLASTp search against the predicted proteome of *B. tabaci* MEAM1 using G4 (BTA021638.1) retrieved from the *B. tabaci* MED protein database as query. This resulted in one nearly (99%) identical hit (Bta08784). The open reading frame of *G4* (*Bta08784*) contains 804 nucleotides (Supplementary Fig. S1) encoding a 267-amino acid protein, including an N-terminal signal peptide of 23 amino acids (likelihood of 0.96). A BLASTp search against the NCBI database (nonredundant proteins for all organisms) only resulted in hits with *B. tabaci*, indicating this effector is specific for whiteflies. Using LOCALIZER, which specifically predicts where eukaryotic effector proteins will localize in plant cells (Sperschneider et al. 2017), the mature G4 protein was not predicted to be in the chloroplast, mitochondrion, or nucleus. However, WolfPsort predicted a nuclear-cytoplasmic localization for the G4 protein. Based on previously obtained *B. tabaci* transcriptomic data (Lee et al. 2018; van Kleeff et al. 2023), G4 is highly expressed in the salivary glands of adult whiteflies, yet it is not expressed during the nymphal stages. Very recently, G4 was identified as a potential virulence (disease-causing) effector with a virus-induced virulence effector (VIVE) assay. This VIVE assay uses the potato virus X vector to transiently express candidate effector genes while following the viral symptoms. Expression of *G4/BTA021638* showed an increase of viral RNA. However, this study contains some uncertainties, as there is a discrepancy between the *B. tabaci* gene ID in Figure 3 (panel c) of that article and the *B. tabaci* gene ID mentioned in the discussion section of that study (Shi et al. 2020).

Yeast two-hybrid (Y2H) screens identified two distinct *S. lycopersicum* target proteins of G4

To analyze whether G4 can directly interact with proteins in tomato, a LexA Y2H screen was performed with G4 (excluding its native signal peptide) as bait in yeast transformed with a cDNA library of *S. lycopersicum* (Hybrigenics Services, Paris, France, https://www.hybrigenics-services.com). A total of 94.1 million clones were screened and subsequently 253 His+ colonies were selected. This resulted in 52 primary candidates. A selection of the candidate target proteins was made based on: (i) (very) high confidence of interaction in the Y2H screen; (ii) putative role in immune suppression/stress response as described in literature; (iii) presence in phloem exudates; or (iv) the homolog in other plant species was a target of pathogen effectors that have been previously published. This led to a list of six candidate targets: Solyc01g099770.2 (MIPDB141); Solyc05g015390.2.1 (RSP1); Solyc10g045380.1.1 (Vacuolar protein sorting protein 62); Solyc02g067390.2.1 (RNA recognition motif containing protein); Solyc07g006280.2.1 (Senescence-associated protein; Tetraspanin); and Solyc08g074290.2.1 (BRI1-KD interacting protein 129). The interactions between preys and effector G4 were confirmed by a 1-by-1 Y2H-interaction assay (Supplementary Fig. S4; Hybrigenics Services).

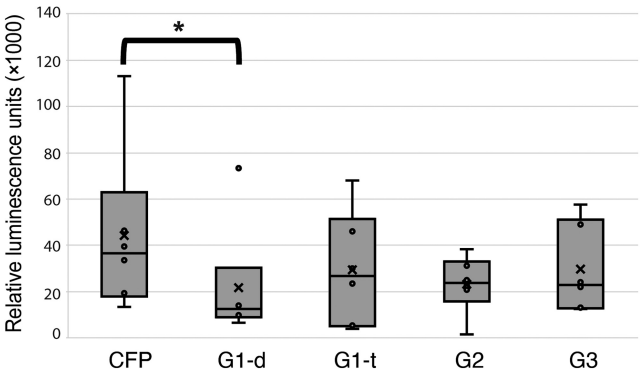

Fig. 1. Reactive oxygen species (ROS) assays with candidate whitefly effectors. Relative luminescence, representing ROS production during a flg22-induced assay in *Nicotiana benthamiana* transiently expressing candidate effectors G1, G2, and G3. CFP, cyan fluorescent protein as control; G1-d, G1 identified in artificial diet; G1-t, G1 identified in transcriptomic data. Asterisk (*$P < 0.05$) indicates a significant difference compared with the CFP control shown by Friedman test (not normally distributed). Box plots represents relative luminescence units (RLU) produced by six plants. Box shows the upper and lower quartiles; whiskers show the minimum and maximum data point within 1.5× interquartile range. Line within the box marks the median; × marks the mean.

Proteomics of phloem exudates confirmed the presence of MIPDB141 in tomato

To determine whether these target proteins were present in the phloem, which supports the probability of interaction in the host, and to analyze whether whiteflies affect the presence of these proteins, phloem exudates were collected from *S. lycopersicum* leaves infested with whiteflies and clean control leaves. MIPDB141 was detected in phloem exudates of both whitefly-infested as well as control plants (Supplementary Table S4). In the phloem of noninfested leaves, the MIPDB141 paralog (Solyc01g099780.2.1) TCTP was also found (Supplementary Table S4), while this was not the case in the infested leaves. RSP1 was not detected in any of the phloem samples. In addition, we analyzed whether the candidate effector proteins identified in the artificial diet were detected in the phloem, and although many other whitefly proteins could be detected in the phloem exudates (data not shown), none of these proteins could be linked to the salivary proteins described in this study.

Luciferase complementation assays confirmed interaction of G4 with both targets

To determine whether the interaction between G4 and the six selected targets could also be observed in planta, a luciferase complementation assay was performed with full-length plant proteins in *N. benthamiana*. Only RSP1 and MIPDB141 resulted in a significantly increased luciferase signal (Fig. 3). In addition, we aligned the amino acid sequences encoded by the partial cDNAs of *MIPDB141* shown to interact with G4 in the Y2H screen. The overlapping region was also cloned and expressed for analysis of the interaction with G4 using the luciferase assay (this part of sequence is indicated in Supplementary Figs. S1 and S2). This was done to determine whether this region in MIPD141 interacts with G4. A significantly increased signal was observed with this part of the MIPDB141 protein, confirming that an interacting site is located in this region. In addition, an increased luciferase signal was detected when G4 fused to either one or the other luciferin part was co-infiltrated, indicating that G4 interacts with itself as well (Fig. 3).

Co-immunoprecipitation (co-IP) confirmed the interaction between G4 and RSP1

To further confirm the interaction in planta between G4 and MIPDB141 and between G4 and RSP1, co-IP assays were performed. All expressed proteins were detected in the input samples before green fluorescent protein immunoprecipitation (GFP-IP), using tag-specific antibodies (Fig. 4). MIPDB141 was

not detected with the GFP-IP in combination G4 fused to GFP, indicating the interaction could not be further established with this assay (Fig. 4A). RSP1 was only detected in the GFP-IP when GFP was fused with G4, with a faint signal indicating a weak interaction between G4 and RSP1.

Subcellular localization and colocalization

To determine where G4 and the target proteins MIPDB141 and RSP1 localize in the plant cell, a subcellular localization study of G4 fused either C- or N-terminally to CFP or red fluorescent protein (RFP) and MIPDB141 and RSP1 fused C- or N-terminally to RFP was performed when transiently expressed in *N. benthamiana* leaves. With all four constructs, the localization of G4 was observed in the cytoplasm, possibly accumulating in the endoplasmic reticulum (ER) and observed surrounding the nucleus, but not in the nucleus (Fig. 5A). The proteins that could be confirmed as interactors in planta using the luciferase complementation assay were further analyzed for their subcellular localization as well. MIPDB141 showed accumulation in the cytoplasm and nucleus, excluding the nucleolus (Fig. 5B). The localization of the candidate target protein RSP1 was determined in the cytoplasm, sometimes seen in a scattered pattern (Fig. 5B). To determine whether the candidate targets were localized in the same cell compartments as G4, a colocalization assay was performed (Fig. 6). MIPDB141 colocalized with G4, but not in the nucleus. There was no indication that G4 may play a role in inhibiting movement of MIPDB141 into the nucleus. RSP1 fused to RFP clearly showed colocalization with G4 fused to CFP. None of the target proteins showed a different localization as result of co-expression with G4.

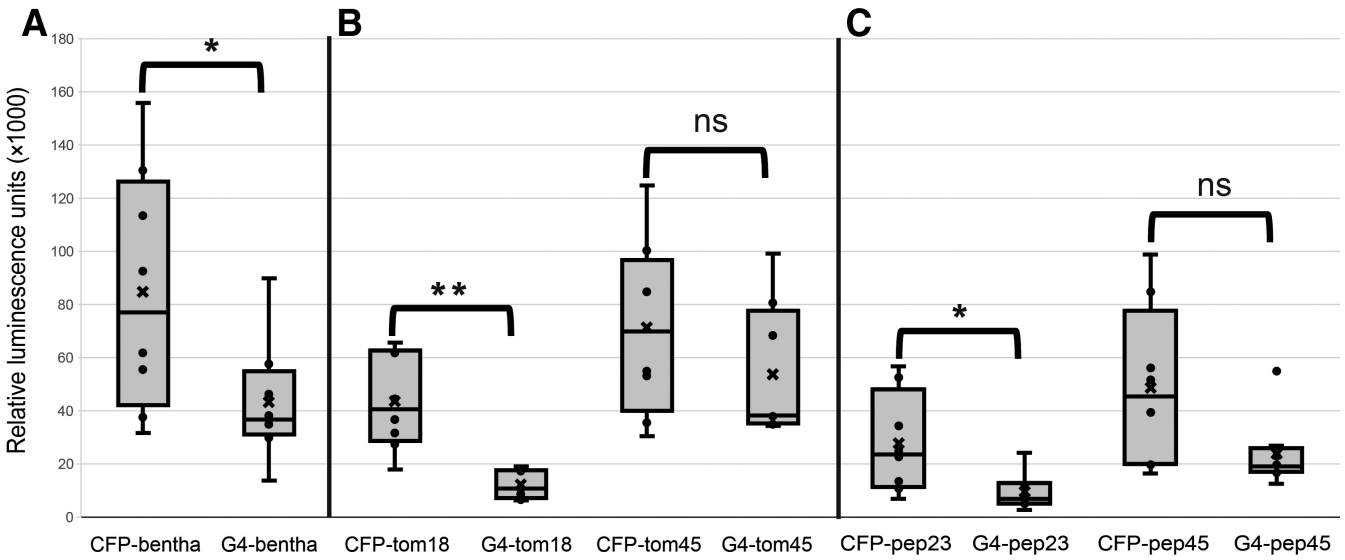

Fig. 2. Reactive oxygen species (ROS) assays with effector G4 in different plant species. Relative luminescence during a flg22-induced ROS assay in *Nicotiana benthamiana*, *Solanum lycopersicum* ('Moneymaker'), and *Capsicum annuum* transiently expressing G4. **A,** ROS production in *N. benthamiana* was analyzed 45 min after induction, showing a significant reduction in ROS production. **B,** ROS production in *S. lycopersicum* was analyzed 18 and 45 min after induction. **C,** ROS production in *C. annuum* was analyzed after 23 and 45 min. CFP, cyan fluorescent protein as control. Asterisks (*$P < 0.05$; **$P < 0.01$) indicate a significant difference compared with the CFP control shown by paired *t*-test or Mann-Whitney *U*-test when the data were not normally distributed; ns indicates nonsignificant difference compared with CFP control. Box plots represents relative luminescence units (RLU) produced by eight plants. Box shows the upper and lower quartiles; whiskers show the minimum and maximum data point within 1.5× interquartile range. Line within box marks the median; × marks the mean.

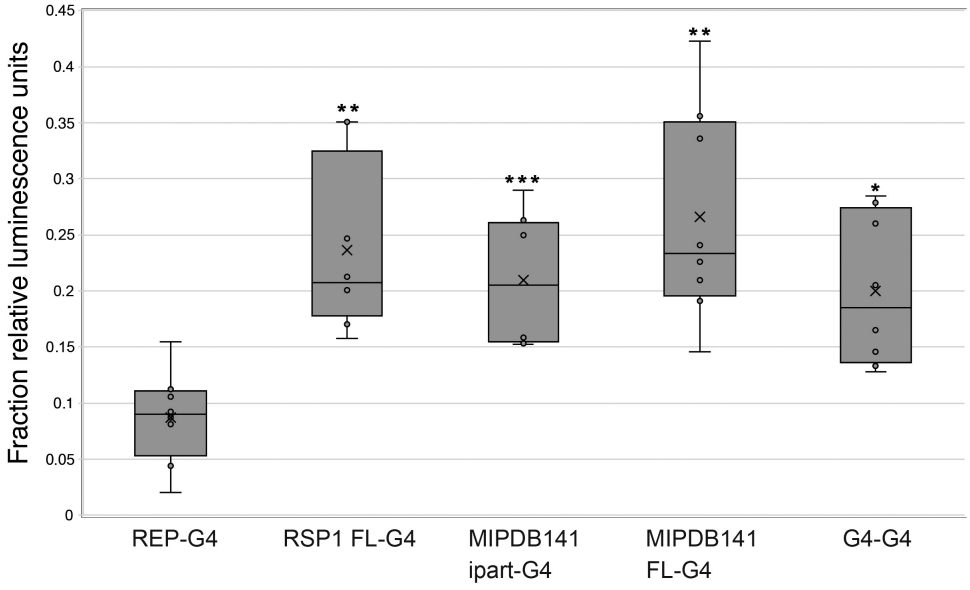

Fig. 3. Confirmation of interaction of G4 with target plant proteins RSP1 (Solyc05g015390: REF-like related stress protein 1) and MIPDB141 (Solyc01g099770; Meloidogyne-induced giant cell protein DB141) using a luciferase complementation assay. REP-G4, negative control; FL, full-length coding sequence; ipart, interacting part (Supplementary Fig. S1). Asterisks (*$P < 0.05$; **$P < 0.01$; ***$P < 0.001$) indicate a significant difference compared with the negative control shown by repeated-measures analysis of variance (ANOVA). Box plots represents the fraction of relative luminescence units (RLU) produced by eight plants. Box shows the upper and lower quartiles; whiskers show the minimum and maximum data point within 1.5× interquartile range. Line within box marks the median; × indicates the mean.

In planta expression of *G4* did not result in an altered whitefly performance

To determine whether presence of effector G4 in planta would influence whitefly performance, we transiently expressed *G4* in *N. tabacum* and *S. lycopersicum* and analyzed oviposition over 3 days. In both plant species, the oviposition of the whiteflies was not significantly different compared with the *CFP* control group (Supplementary Fig. S5).

Virus-induced gene silencing (VIGS) of *MIPDB141* affects whitefly performance

To determine whether the target gene *MIPDB141* plays a significant role in the whitefly–plant interaction, we reduced its expression in *S. lycopersicum* and assessed whether this affected whitefly performance. Concomitantly, the *MIPDB141* paralog (Solyc01g099780.2.1; TCTP) was also targeted by the VIGS constructs, as it was impossible to design a paralog-selective construct. We selected *MIPDB141/TCTP*-silenced leaves based on the photobleaching in *phytoene desaturase* (*PDS*)-silenced plants. Using specific primers, partly designed on the UTR, we could confirm that both genes were significantly silenced in *S. lycopersicum* leaflets (Fig. 7C). Disks were taken and infested with female whiteflies for 2 days to allow oviposition. After 2 days, the number of eggs per living female was significantly lower on the *MIPDB141/TCTP*-silenced plants compared with the *GFP* control (Fig. 7A). Because reduced oviposition was observed on the *MIPDB141/TCTP*-silenced leaf disks, a bioassay combining silenced and control leaf disks was performed to determine whether reduced oviposition could be caused by a lower attractiveness of the *MIPDB141/TCTP*-silenced leaf disks. Unexpectedly, we observed that adult females were significantly more attracted to the *MIPDB141/TCTP*-silenced leaf disks than to the *GFP* control (Fig. 7B).

Discussion

Here we have shown that the effector protein G4 impairs tomato immunity to whiteflies by interfering with an elicitor-induced ROS response and via a direct interaction with tomato susceptibility protein MIPDB141. Considering the number of plant proteins identified in the Y2H, G4 might also target other plant proteins. The interaction with TCTP, a paralog of MIPDB141, is likely to occur in the host plant, because of the high similarity and identification in the Y2H screen. We have also confirmed the interaction between RSP1 and G4 in planta. The identification and characterization of effectors used by herbivorous pests to manipulate the physiology of their host is an essential element for understanding the mechanisms that drive the ecology and evolution of plant–insect interactions. Moreover, elucidation of effector targets in host plants offers novel opportunities for resistance breeding to improve crop resilience, for example, via knockout or mutagenesis of targets (Bisht et al. 2019; Vleeshouwers and Oliver 2014). The identified G4 targets in *S. lycopersicum* are potential breeding targets to improve whitefly resistance in crops. In theory, if the interaction site in the plant protein can be modified to disrupt the interaction with G4 while maintaining its normal function, this will lead to higher resistance levels.

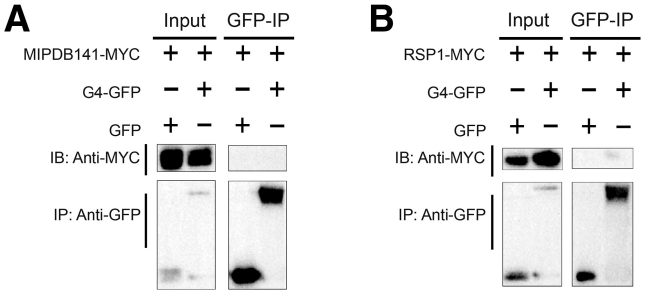

Fig. 4. Co-immunoprecipitation assays of G4 with MIPDB141 and RSP1 in *Nicotiana tabacum*. **A,** MIPDB141 fused to MYC-tag was co-expressed with either G4 fused to green fluorescent protein (GFP) or free GFP. Proteins were expressed and detected in the protein extract. MIPDB141 was not detected in the GFP-IP either with free GFP or G4 fused to GFP. **B,** RSP1 fused to MYC-tag was co-expressed with either G4 fused to GFP or free GFP. Proteins were expressed and detected in the protein extract. RSP1 was detected in the GFP-IP when co-expressed with G4 fused to GFP, but not with free GFP. IP, immunoprecipitate; IB, immunoblot.

In previous studies, different methods were successfully used to identify effectors of insect pests like *B. tabaci* (reviewed in Naalden et al. 2021). In this study, we used an artificial diet as a food source for whiteflies as a direct approach for harvesting salivary proteins secreted via their stylets into their diet while feeding. Previously, this was successfully applied for identifying salivary proteins of spider mites (Jonckheere et al. 2016) and several insect species, including whiteflies (Huang et al. 2021; Yang et al. 2017). We were able to identify several proteins that qualify as candidate salivary effectors of *B. tabaci.* Of particular note, these proteins were previously also detected in artificial diet by Huang et al. (2021), indicating a robust secretion of these proteins by whiteflies.

To assess whether our candidate effectors are secreted in the phloem, we collected phloem exudates of whitefly-infested *S. lycopersicum* leaves, but none of the candidates reported here could be detected. Possibly some whitefly salivary proteins might have moved to, or even beyond, phloem companion cells as is seen, for example, with phytoplasma effectors (reviewed in Jiang et al. 2019) or have a relatively short half-life after injection into the plant. Alternatively, the effector proteins identified from artificial diet might be specifically secreted by adult whiteflies, while for collection of the phloem exudates, which takes several hours, adult whiteflies had been removed and only nymphs and eggs were present. Accordingly, van Kleeff et al. (2023) could identify only one whitefly effector candidate in phloem exudates, and its corresponding gene was specifically expressed in nymphs and eggs. Hence, a different setup that does not exclude feeding adults during phloem extraction may give a better view on the whitefly salivary proteins injected during feeding.

Modulation of defense responses

Plants defend themselves against herbivores in various ways. The production of ROS is a central defense-related response in plants under attack, as ROS are important defense signals as well as toxic components for many insects (Goggin and Fischer 2021; Kerchev et al. 2012). For example, sugarcane aphids induce ROS production in sorghum and an H_2O_2 accumulation directly increases plant resistance against the aphid in different sorghum genotypes (Pant and Huang 2021). In addition, feeding by whitefly nymphs resulted in upregulation of several genes in *Arabidopsis thaliana* involved in scavenging of ROS and redox homeostasis, suggesting that nymphs induce ROS accumulation (Kempema et al. 2007). In this study, we performed ROS induction assays to identify effectors that can suppress this response. Assays with G3 did not result in a significant reduction of ROS induction. However, Peng et al. (2023) showed that G3, which they called BtE3, was able to suppress the *B. glumae*-induced HR in *N. benthamiana* and tomato. In addition, it plays a role in activation of the salicylic acid (SA)-signaling pathway and repression of the JA-signaling pathway (Peng et al. 2023). Thus, G3 might have distinct roles in the host during defense. In addition, assays with G1 did suppress the production of ROS but not always to a significant level. This candidate effector may have an interesting role in immune modulation as well and may in

fact be related to other early defense induction pathways. For example, Bsp7 has 60% identity with G1 and is able to reduce the DAMP-induced plant immunity in *N. benthamiana* (Wang et al. 2019).

G4 acted as a robust ROS suppressor, indicating that this protein is an effector that modulates the early immune response of the host during the whitefly–plant interaction. G4 consistently suppressed ROS in *N. benthamiana*, while it delayed the ROS accumulation dynamics in *S. lycopersicum* and *C. annuum*. These different effects on the ROS accumulation dynamics of different plant species could have many causes, such as differences in interaction strength between G4 and target orthologs, but on the

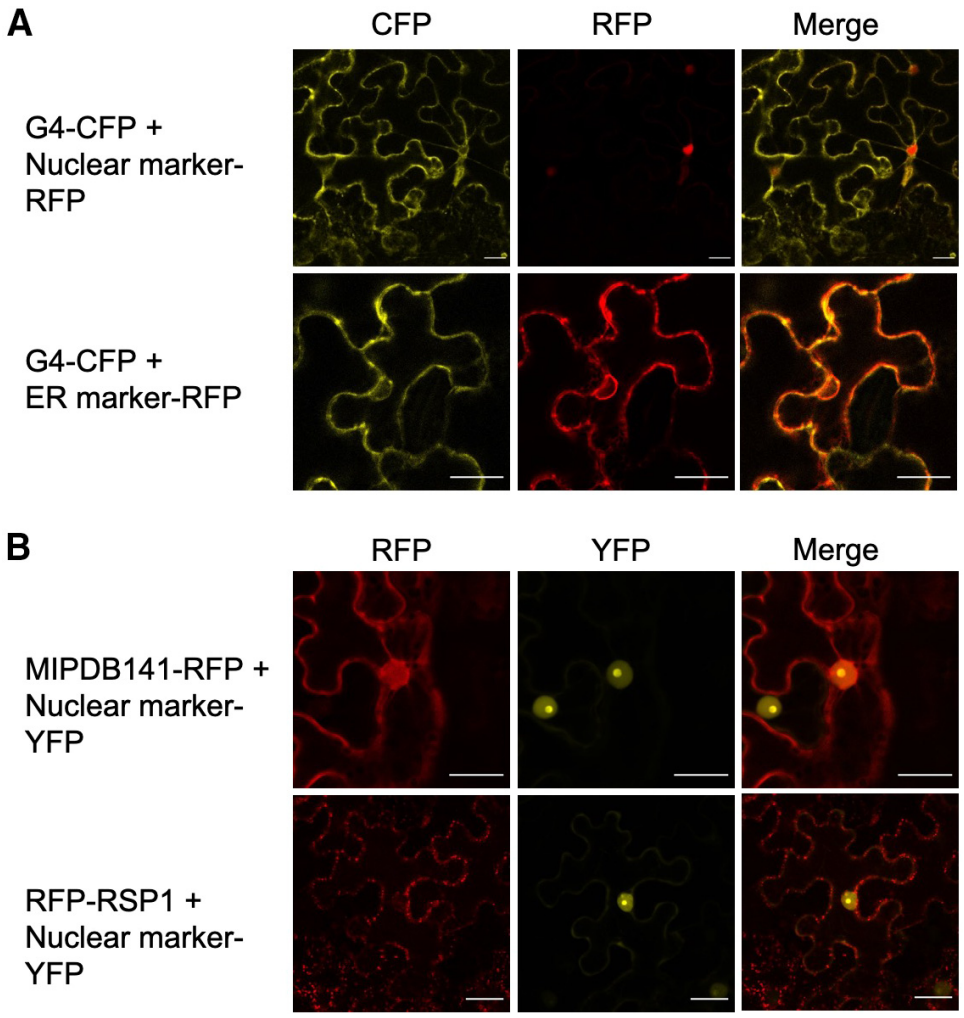

Fig. 5. Subcellular localization of G4, RSP1, and MIPDB141 in *Nicotiana benthamiana* leaves. **A,** G4 was imaged in presence of a nuclear marker (3xNLS-RFP) or luminal endoplasmic reticulum (ER) marker (HDEL-RFP), showing localization predominantly in the ER. **B,** Target plant proteins MIPDB141 and RSP1 were imaged in the presence of a nuclear marker (3xNLS-YFP). MIPDB141 localized in the cytoplasm and nucleus, excluding the nucleolus. RSP1 localized in the cytoplasm in a scattered pattern. CFP, cyan fluorescent protein; RFP, red fluorescent protein; YFP, yellow fluorescent protein. Scale bar: 25 μm.

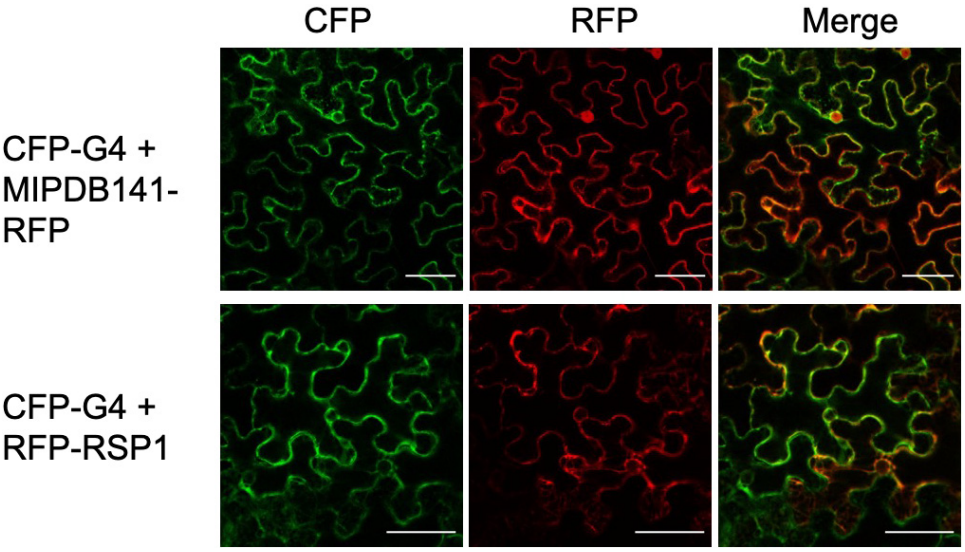

Fig. 6. Subcellular colocalization of G4 with RSP1 and MIPDB141 in *Nicotiana benthamiana* leaves. MIPDB141 colocalized with G4 in the cytoplasm/endoplasmic reticulum (ER), but not in the nucleus. RSP1 colocalized with G4 in the cytoplasm. CFP, cyan fluorescent protein; RFP, red fluorescent protein. Scale bar: 25 μm.

other hand, they may just be a direct result of lower expression in *S. lycopersicum*. Direct expression of G4 in planta did not affect whitefly performance. We hypothesize that this might be related to the high expression of this gene in the whitefly glands. The amount of G4 secreted by the whitefly may result in maximum suppression of the specific pathway targeted and, hence, is not affected by the additional amount of G4 protein expressed by the host.

Interaction with plant proteins

Two target proteins of G4 in *S. lycopersicum*, RSP1 and MIPDB141, were identified in this study using a tomato cDNA library in yeast and were subsequently confirmed independently via in planta interaction assays. Concomitantly, the biological relevance of the G4-MIPDB141 interaction was confirmed via VIGS in *S. lycopersicum*. Functional interactions of pathogen effectors with multiple host targets have been reported before (Pennington et al. 2016). Also, the whitefly orthologous effectors Bt56 and Bsp9 from *B. tabaci* MED and MEAM1, respectively, were found to interact with two distinct plant proteins, but it was confirmed in yeast that Bsp9 also interacts with the Bt56 plant target KNOTTED 1-like homeobox transcription factor (NTH202), supporting the idea that whitefly effectors can have multiple targets in the host plant (Wang et al. 2019; Xu et al. 2019). We confirmed the interactions between G4 and the two plant targets in planta independently using the luciferase complementation assay. This is a relatively easy technique for screening interactions in plant tissue and confirms interacting proteins are accumulating in the same cell compartment(s). Furthermore, using Co-IP as another independent assay, we could confirm the interaction between RSP1 and G4. Co-IP is especially suitable for relatively strong interactions (Struk et al. 2019). The interaction between MIPDB141 and G4 is probably relatively weak, as it was not observed in the Co-IP but was confirmed in the Y2H and luciferase complementation assay, techniques suitable for the confirmation of relatively weak interactions. Altogether, we identified RSP1 and MIPDB141 to be in planta target proteins of G4. In addition, with the confirmed interaction between G4 and the overlapping MIPDB141 fragment of the different truncated preys from the Y2H screen (Supplementary Figs. S1 and S2), we could narrow down the interesting region for gene modification and further resistance breeding.

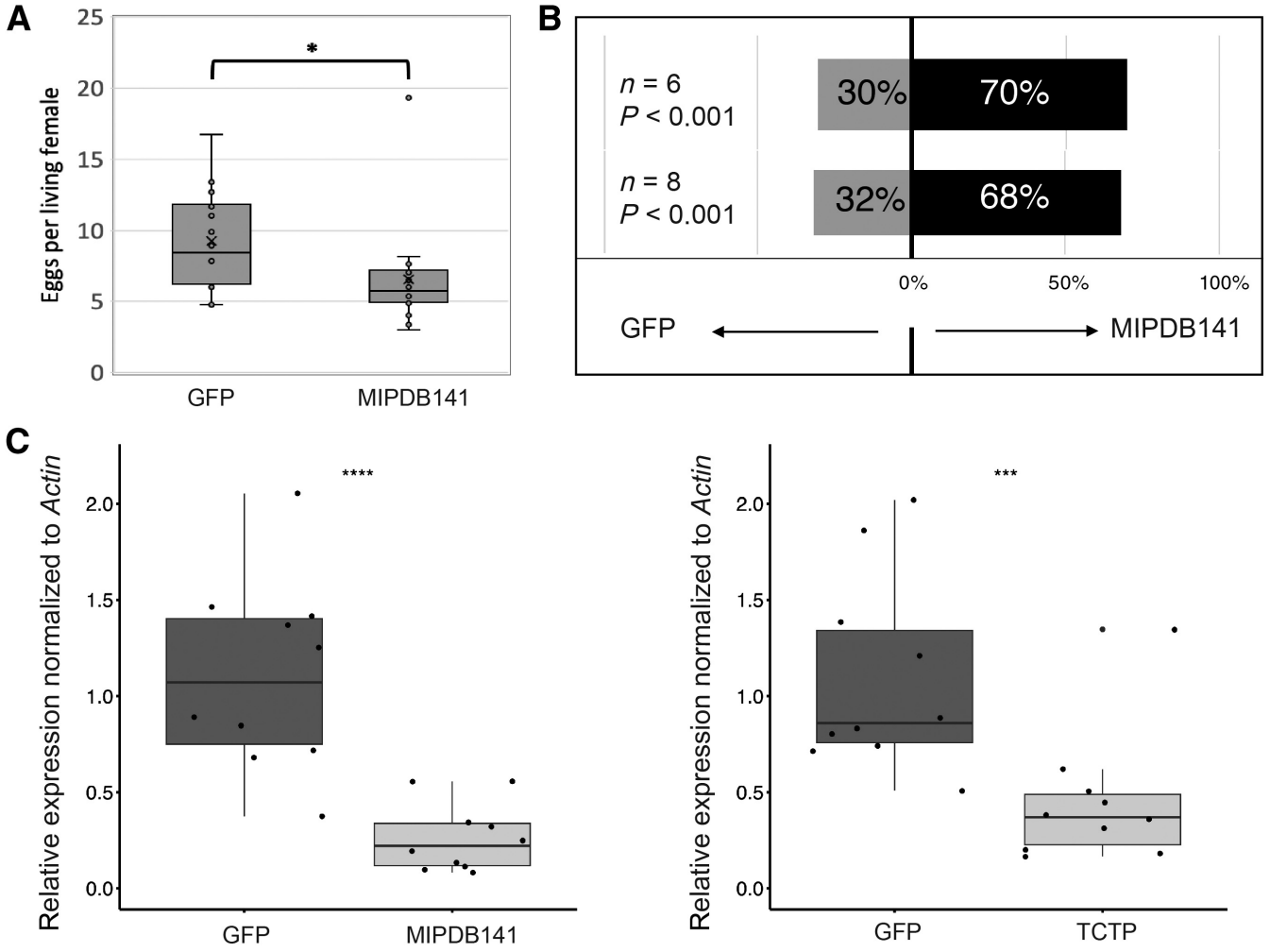

Fig. 7. Virus-induced gene silencing (VIGS) whitefly bioassays on *Solanum lycopersicum* ('Moneymaker') with dsRNA produced against green fluorescent protein (*GFP*; negative control) or *MIPDB141*. **A,** Number of eggs deposited by whiteflies in a non-choice assay after 2 days of oviposition ($n = 16$). Box plots represents eggs per living female on 16 plants. Box shows the upper and lower quartiles; whiskers show the minimum and maximum data point within 1.5× interquartile range. Line within box marks the median; × marks the mean. Asterisk ($*P < 0.05$) indicates a significant difference compared with the GFP control shown, using a factorial analysis of variance (ANOVA). **B,** Percentage of whiteflies that selected the *GFP*-silenced plants or the *MIPDB141*-silenced plants in a choice assay conducted twice independently. To determine significant difference, a replicated *G*-test for goodness of fit was used. **C,** Expression levels of *MIPDB141* and *TCTP* in VIGS-treated leaf tissue relative to *Actin*. Asterisks ($****P < 0.0001$; $***P < 0.001$) indicate a significant difference compared with the *GFP*-silenced control plants by Mann-Whitney *U*-tests.

MIPDB141 and other TCTPs are highly conserved and have been identified in all eukaryotic organisms (Bommer and Thiele 2004). They are involved in many cellular processes, like growth and development and (a)biotic stress responses (reviewed in Deng et al. 2016). Transcriptome analysis of root-knot nematode-induced giant cells showed an upregulation of *MIPDB141*, indicating a role in nematode–plant interaction (Bird and Wilson 1994). We were able to detect MIPDB141 in the phloem exudates of *S. lycopersicum*. TCTPs have also been detected in phloem sap in previous studies in different plant species like *Cucurbita maxima* (Aoki et al. 2005) and *A. thaliana* (Berkowitz et al. 2008). Because whiteflies in general are believed to secrete most of their effectors into the sieve tubes of the phloem, this provides strong support that a MIPDB141–G4 interaction in planta might indeed occur in the vascular bundle and/or its companion cells. Interestingly, Deng et al. (2016) showed that the MIPDB141 ortholog of *Hevea brasiliensis* (HbTCTP1) interacts with HbRSP1, its homolog of RSP1 in *S. lycopersicum*. Whether MIPDB141 and RSP1 also interact in *S. lycopersicum* is unknown, but given the high degree of conservation of these proteins, it is likely that this interaction occurs as well. Because G4 interacts with both MIPDB141 and RSP1—and with itself—the three proteins may form a complex together, and G4 may possibly influence the interaction between MIPDB141 and RSP1. (Co)localization studies show that G4 and the two target proteins all localize to the cytosol but that MIPDB141 also localizes to the nucleus. It suggests that the interaction between the target proteins with G4 takes place exclusively in the cytosol and that G4 does not seem to influence localization of MIPDB141 to the nucleus nor does it colocalize with MIPDB141 in the nucleus. Interestingly, both G4 and RSP1 did not localize in the nucleus, although both proteins (including fluorescent tag) are sufficiently small to diffuse to the nucleus (Wang and Brattain 2007). The fact that we did not detect RSP1 in the phloem exudates may be explained by accumulation of RSP1 in the companion cells, where effectors may also be translocated after secretion. In addition, RSP1 may be present in low amounts or only present during certain stress responses. Whether this is the case or whether the localization of G4 and RSP1 is in the phloem or in the companion cells could be further investigated using immunolocalization. For example, immunolocalization for the whitefly effector Bt-Fer1 shows that it localizes to the phloem (Su et al. 2019).

REF-like proteins in *H. brasiliensis*, orthologs of tomato RSP1, are stress-related proteins (Ko et al. 2003), which indicates that the interaction with G4 involves modulating the stress response in the plant tissue. TCTPs are highly conserved, and many functions in the cell are attributed to these proteins, but there are relatively few in planta studies regarding TCTPs compared with studies in animal tissues or cell lines (Deng et al. 2016). This makes it challenging to predict the effect of G4 binding to MIPDB141 in plant tissues. *HbTCTP1* in *H. brasiliensis* was shown to be regulated by several stress conditions, including drought, wounding, and H_2O_2 treatment (Deng et al. 2016), while overexpression of *AtTCTP* in *N. benthamiana* resulted in a decrease in cell death (Hoepflinger et al. 2013). Plants in general contain one to three different TCTP paralogs (Gutiérrez-Galeano et al. 2014). In tomato, two TCTPs are present: MIPDB141 and Solyc01g099780.2. In our VIGS assay, we interfered with transcript accumulation of both paralogs, possibly preventing functional redundancy that could undo the effect of silencing. In the Y2H screen, the main prey found was MIPDB141, although one of the identified preys was Solyc01g099780.2. The fact that the paralog was found only once may reflect underrepresentation of this transcript in the (unnormalized) cDNA library that had been used for the Y2H screen. The fact that both genes have been identified in the Y2H screen strongly suggests that G4 interacts with the two paralogs in tomato simultaneously, as both are expressed in the same tissues under similar conditions (Tomato Expression Atlas, https://tea.solgenomics.net). Therefore, the reduced whitefly fecundity observed in the VIGS assay is a result of the simultaneous silencing of both genes. In future research, it would be interesting to further explore whether both targets are equally important and whether mutations in one of the two could lead to an increased resistance against whiteflies.

Whitefly choice and no-choice bioassays

The choice assay showed that whiteflies preferred the *MIPDB141*-silenced leaf disks. Yet during the no-choice bioassay on *MIPDB141*-silenced leaf disks, their oviposition was reduced relative to the control group, confirming the insect needs MIPDB141 for optimal performance. This points to a puzzling role for MIPDB141 in interacting with the whitefly and suggests that its foraging behavior is influenced in the opposite way as its oviposition behavior. At a minimum, we show here that the reduced number of eggs found on the *MIPDB141*-silenced leaf disks is not a direct result of whiteflies repelled by this plant tissue. Assuming the G4-MIPDB141 interaction is adaptive to the whitefly, it may under natural circumstances never encounter plants without *MIPDB141* expression. Therefore, silencing this gene may generate irrelevant pleiotropic cues that influence foraging or oviposition behavior in an unnatural manner. So, from a biological point of view this result may not be very relevant. More important is that the whitefly benefits from the presence of MIPDB141 in the plant tissue. For breeding purposes, simply knocking the gene out may not be suitable for obtaining resistant crops, because this conserved gene has several primary functions in the plant (Berkowitz et al. 2008; Hoepflinger et al. 2013), while according to our data, it may make the plant more attractive to whiteflies, possibly negating the beneficial effect via oviposition reduction. Thus, the challenge will be to identify alternative MIPDB141 alleles, either from natural (resistant) plant populations or via mutagenesis, that encode for MIPDB141 proteins that do not interact with G4, thereby reducing whitefly performance, but retain their primary function. These plants most likely will not attract whiteflies more strongly. Stacking such alleles in crops could be very valuable for breeding programs that aim for sustainable insect resistance.

In conclusion, in this study, we identified and functionally analyzed the whitefly effector G4. We demonstrate that G4 is an immune response-modulating protein that interacts with two host proteins of *S. lycopersicum*. These findings provide more insight into how whiteflies are able to hijack the physiology of the plant. The identified host targets may be interesting for further development of resistance against whiteflies.

Materials and Methods

Rearing *B. tabaci*

The *B. tabaci* strain (MED, Q-biotype), used for saliva collection, was initially sampled from greenhouse-cultivated eggplants in Ierapetra, South Crete (Greece) and maintained on cotton plants in a plant growth cabinet at 25 (±1)°C, 50 to 60% relative humidity and a 16/8-h light/dark regime at the Biology Department, University of Crete (Greece). For isolation of effectors and bioassays, the *B. tabaci* population (MEAM1) was maintained on cucumber plants in a greenhouse at 28°C under 16/8-h light/dark regime at the University of Amsterdam.

B. tabaci saliva collection

Petri dishes (55-mm diameter) with two ventilation holes covered with thin mesh on the side walls, were used as feeding chambers. Approximately 200 newly emerged whitefly females were immobilized using CO_2 and placed in a Petri dish. The Petri dish was covered with two layers of Parafilm with 1 ml of arti-

ficial diet containing 30% sucrose and rifampicin (0.05 mg/ml) between the two layers. The feeding chambers were placed in a growth cabinet under a 25 (±1)°C, 50 to 60% relative humidity, and a 16/8-h light/dark regime. Three biological replicates of artificial diet enriched with whitefly saliva were collected (approximately 800 µl of artificial diet/replicate) after 6 and 24 h of whitefly feeding (Btab_6h or Btab_24h). Three replicates of artificial diet without whitefly saliva were collected at the same time points as controls (Con_6h or Con_24h). Collected artificial diet samples were kept at –80°C until further use.

Proteomics of artificial diet

Artificial diet samples were lysed using 200 µl of RIPA lysis buffer (Thermo Fisher Scientific, Belgium) and 1× HALT protease inhibitor (Thermo Fisher Scientific), combined with a 30-s sonication (Branson Sonifier SLPe ultrasonic homogenizer, Labequip, Ontario, Canada) with an amplitude of 50%, on ice. After centrifugation of the samples for 15 min at 10,000 × *g* at 4°C, the pellet was discarded. Next, 1 µg of protein was taken and trypsin digested for liquid chromatography with tandem mass spectrometry (LC-MS/MS) analysis. Digested samples were separated by nano–reverse phase C18 (RP-C18) chromatography on a Waters nano-acquity nano-UPLC system. The liquid chromatograph was connected to a Q-Exactive Plus mass spectrometer equipped with a nanospray ion source (Thermo Fisher, Waltham, MA, U.S.A.). The high-resolution mass spectrometer was set up in an MS/MS mode, where a full-scan spectrum was followed by a high-energy collision-activated dissociation tandem mass spectra. Peak lists obtained from MS/MS spectra were identified using different algorithms embedded in SearchGUI (version 3.3.16) (Vaudel et al. 2011) and a concatenated target/decoy version of the *B. tabaci* MED protein database. Peptides and proteins were inferred from the spectrum identification results using PeptideShaker version 1.16.42 (Vaudel et al. 2015). Peptide spectrum matches, peptides, and proteins were validated at a 1.0% false discovery rate (FDR) estimated using the decoy hit distribution. Only those proteins that were identified in at least two out of three biological replicates and not in any control sample were regarded as present and reliably identified (see the Supplementary Material for a detailed description of the LC-MS/MS [Supplementary Method S1] and proteomics data [Supplementary Method S2] analyses). The mass spectrometry data along with the identification results have been deposited to the ProteomeXchange Consortium (Vizcaíno et al. 2014) via the PRIDE partner repository (Martens et al. 2005) with the dataset identifiers PXD033180 and 10.6019/PXD033180. The presence of a signal peptide in the detected *B. tabaci* proteins was predicted using SignalP version 6.0 (Teufel et al. 2022).

Sequence analysis of G4

The coding region of G4 (*BTA021638)* was used in a BLASTp search against the Whitefly Genome Database (MEAM1; http://www.whiteflygenomics.org/cgi-bin/bta/index.cgi; Chen et al. 2016) and the nonredundant protein and nucleotide databases for all organisms (highly similar sequences [megablast] of the NCBI). Protein alignments were made using the ClustalW multiple alignment algorithm in Bioedit sequence alignment editor (Hall 1999). Prediction of cellular localization was performed using Wolf PSort (https://wolfpsort.hgc.jp) and LOCALIZER (https://localizer.csiro.au; Sperschneider et al. 2017) using the mature G4 sequence (without signal peptide) as input. Prediction of domains was performed using InterPro (https://www.ebi.ac.uk/interpro; Paysan-Lafosse et al. 2023).

Plant growth

Seeds of *N. benthamiana*, *Nicotiana tabacum*, *S. lycopersicum* ('Moneymaker'), and *Capsicum annuum* ('Mandy') were germinated in soil at 21°C and 16/8-h light/dark regime at 65% relative humidity and circa 1-week-old individual plantlets were transferred to pots. The plantlets were grown for 4 to 5 weeks before *Agrobacterium tumefaciens* infiltration, ROS assays, phloem extraction, and bioassays. For the VIGS assays, 9-day-old *S. lycopersicum* plantlets were agroinfiltrated and kept under the same conditions post-agroinfiltration.

Cloning procedure

Effector and plant protein constructs. Full-length coding sequences of the candidate effectors were PCR amplified from *B. tabaci* MEAM1 cDNA (adult stage; G1-transcriptome [G1-t], G3, and G4) using gene-specific primers (primers are listed in Supplementary Table S5). Effector G2 and G1-diet (G1-d) sequences were retrieved from the Whitefly Genome Database (MEAM1; http://www.whiteflygenomics.org/cgi-bin/bta/index.cgi; Chen et al. 2016) and were synthesized without signal peptide, and flanked by attLR1 and attLR2 cloning sites at GeneUniversal (Newark, DE, https://www.geneuniversal.com) in vector pUC57. Coding sequences of G4 interacting proteins *MIPDB141* (*Meloidogyne-induced giant cell protein DB141*; *Solyc01g099770.2*) and *RSP1* (*REF-like stress related protein 1*; *Solyc05g015390.2.1*) were retrieved from the Sol Genomics Network (SGN) database (Fernandez-Pozo et al. 2015), synthesized at GeneUniversal in vector PUC57. The sequence part of *MIPDB141* that was overlapping among the different partial cDNA clones (preys) interacting with G4 in the Y2H screen was synthesized as well in vector PUC57 (Supplementary Fig. S1). The design of the VIGS construct was conducted using the Sol genomics VIGS tool (https://vigs.solgenomics.net) with the database *Solanum lycopersicum* ITAG v2.40. The fragment sequences were synthesized at GeneUniversal as described above. The VIGS construct was covering partly the mRNA of the genes *Solyc01g099770* and *Solyc01g099780* (Fig. 1; see the Supplementary Material). Final constructs were verified by sequencing. Constructs were either transformed into *A. tumefaciens* strain GV3101 using the freeze–thaw method described in Holsters et al. (1978) for agroinfiltration in *N. benthamiana*, *N. tabacum*, and VIGS in *S. lycopersicum* or in *A. tumefaciens* strain 1D1249 for agroinfiltration of *S. lycopersicum* and *C. annuum* for ROS and bioassays.

Nuclear marker (colocalization). The pGWB541-3xNLS-YFP plasmid was constructed by synthesizing attL1-3xNLS-attL2 (attL1-MGLRSRADPKKKRKVDPKKKRKVDPKKKRKVGSTGSR-attL2) by Gene Universal (https://www.geneuniversal.com) followed by Gateway LR clonase reaction (Thermo Fisher Scientific) into the pGWB541 (C-terminal YFP) destination vector (Nakagawa et al. 2007).

Modification of the destination vectors for luciferase complementary assay. A red-shifted version of the firefly luciferase gene having the mutation I288A (Wang et al. 2013) was *A. thaliana* codon optimized, synthetized (Eurofins genomics; for coding sequence, see Supplementary Fig. S1), and cloned into destination vector pGWB402 (Nakamura et al. 2010). The N-terminally tagged luciferase and the empty vector PGWB402 were digested with the restriction enzyme *Xba*I. The C-terminally tagged luciferase and the empty vector PGWB402 were digested with the restriction enzyme *Afe*I. The fragments contain the luciferase coding sequence of amino acids 1 to 398 for the N-terminus and 394 to 550 for the C-terminus (Paulmurugan and Gambhir 2007). The N-terminus was fused in frame to a FLAG-tag and the C-terminus to an HA-tag. The fragments were PCR amplified and inserted in vector pGWB402 by restriction cloning (Nakagawa et al. 2007). This led to the

following vectors for in-frame fusion of the protein of interest pGWB402 HA-RedFFLuc Cterm-Gateway box and pGWB402 Gateway box RedFFLuc Nterm-FLAG-Stop (Supplementary Table S6).

Assay for ROS induced by flg22

Infiltration of *N. benthamiana*. *Agrobacterium* (strain GV3101) carrying either effector constructs or, as negative control, the CFP construct, or the P19 silencer inhibitor construct (pBIN61:P19) (Jay et al. 2023) was grown for 1 to 2 days at 28°C in LB medium supplemented with the appropriate antibiotics. Cells were resuspended in infiltration buffer (2% wt/vol sucrose, 1× Murashige & Skoog Basal Salt Mixture without vitamins [Duchefa Biochemie, The Netherlands]), 10 mM 2-(*N*-morpholino)-ethanesulfonic acid [MES], 200 μM acetosyringone, pH 5.6) to an OD_{600} of 0.6 and incubated for at least 3 h in the dark at room temperature. Before infiltration, the *Agrobacterium* carrying the effector construct and *Agrobacterium* carrying the P19-silencing inhibitor were mixed in a ratio of 1:1. After agroinfiltration, plants were allowed for expression for circa 2 days.

Infiltration of *S. lycopersicum* and *C. annuum*. *Agrobacterium* (strain 1D1249) carrying either an effector construct or, as negative control, the CFP construct was grown for 1 to 2 days at 28°C in LB medium with the appropriate antibiotics. Agrobacteria were pelleted and resuspended in infiltration buffer to an OD_{600} of 0.3. Plant disks of 2.4 mm, including a small part of the petiole, were taken from expanded leaves from 4- to 5-week-old *S. lycopersicum* or *C. annuum* plants. Vacuum agroinfiltration was performed as described in Abd-El-Haliem et al. (2018). Disks were placed in 6-well plates with 0.6% Daishin agar dissolved in MQ water (Duchefa) on the edge of the wells. The petiole of the leaf disks was placed in the agar, and the plastic lid was placed back on the plate. Plates were placed on 25°C under a 16/8-h light/dark regime in a climate cabinet for 3 days.

Luminescence measurement. Leaf disks (16 mm^2) were collected from agroinfiltrated *N. benthamiana*, *S. lycopersicum*, or *C. annuum* areas and transferred to 96-well white plates. Assays were performed for 6 to 8 independent biological replicates (plants), and for each infiltrated disk, two replicates were taken. The leaf disks were floated for 6 to 12 h on 190 μl of autoclaved MQ water for recovery. Just before the luminescence measurement, the water was removed and replaced by a mixture of 100 nM flg22 (QRLSS GLRINSAKDDAAGLAIS; Felix et al. 1999), 0.5 mM luminol probe 8-amino-5-chloro-7-phenyl-pyrido[3,4-d]pyridazine-1,4(2H,3H)dione (L-012) (Wako Chemicals, Richmond, VA, U.S.A.), and 20 μg/ml horseradish peroxidase Type VI-A (Sigma, St. Louis, MO, U.S.A.). ROS production was measured by a luminol-based assay (Keppler et al. 1989) over 45 min with measurement intervals of 2 min with an integration time of 1 s.

Whitefly bioassays

Agroinfiltration of *N. tabacum* and *S. lycopersicum* was performed as described for the ROS assays. After 3 days of expression in *N. tabacum*, a whitefly bioassay was performed as described in van Kleeff et al. (2023). For whitefly bioassays with *S. lycopersicum*, Petri dishes with vents were used with 0.6% agar on one side covered with transparent foil (Supplementary Fig. S6A). The leaf disc was placed through a cut in the foil, allowing for 3 days of expression. The petiole was placed through a cut in the foil in the agar in such way that the leaf disks were sticking out from the side, leaving space for the whiteflies to move to the abaxial side of the leaf disk. White weighing paper was placed at the bottom of the Petri dish to reduce humidity. Whiteflies were collected from cucumber plants by aspiration and placed on ice until they reached a chill coma. Fifteen whitefly females were placed in each Petri dish. Petri dishes were closed and sealed using Leukopore tape and placed in a growth cabinet at 27°C, 70% relative humidity, and a 16/8-h light/dark regime. After 3 days, the Petri dishes with whiteflies were stored at –20°C. Healthy-looking females (undamaged and no morphological changes in color and hydration, similar to whiteflies in chill coma) were considered to be alive just before freezing and were counted as living females.

Yeast two-hybrid screening

A LEXA Y2H screening was performed by Hybrigenics Services with the G4 coding sequence (excluding its native signal peptide) against a cDNA library of leaf, petiole, stem, and root tissue of tomato yellow leaf curl virus (TYLCV)-infected *S. lycopersicum*, constructed into activation domain vector pP6 (TOPLI). G4 was cloned into a LexA DNA-binding domain vector pB27 (N-LexA-G4-C fusion). Obtained prey fragments were sequenced and identified using the NCBI database. The predicted biological score following Formstecher et al. (2005) was used to indicate the confidence of an interaction. Selected preys with very high confidence or high confidence scores were confirmed for interaction by 1-by-1 screening on selective medium (Supplementary Fig. S4). As a negative control, the constructs were combined with empty pB27 vector or empty pP7 vector.

(Co-)localization

Agrobacterium (strain GV3101) carrying various constructs was prepared as described in the section "Assay for ROS Induced by flg22." Agrobacteria were infiltrated together with the P19-silencing inhibitor construct in infiltration buffer with an OD_{600} of 0.5, on the abaxial side of leaves of 4- to 6-week-old *N. benthamiana* plants. Expression was allowed for 3 to 5 days at 21°C under 16/8-h light/dark regime. Imaging of the fluorescence signal was performed with a Nikon Ti A1 confocal microscope using a 20× Plan Fluor, NA 0.75 (multi-immersion) objective. eRFP was excited with a wavelength of 561 nm, and emission was detected at 592 to 632 nm. eCFP was excited with a wavelength of 440 nm, and emission was detected at 465 to 500 nm. eYFP was excited with a wavelength of 514 nm, and emission was detected at 525 to 555 nm. Autofluorescence of chlorophyll was detected at 657 to 737 nm.

Luciferase complementation assay

Agrobacterium (strain GV3101) carrying the desired construct was grown overnight in liquid LB supplemented with the appropriate antibiotics. The liquid cultures were centrifuged and pellets resuspended in infiltration buffer to a final OD_{600} of 0.8 for the luciferase complementary constructs and a final OD_{600} of 0.4 for the P19-silencing inhibitor. As a negative control, effector G4 fused to the N-terminus half of the luciferase was expressed together with $TYLCV^{Alb13}$ Rep (FJ956702.1) (Maio 2019) fused to the C-terminus half of the luciferase. Expression was allowed for 3 days postinfiltration. Leaves were brushed two times with D-luciferin buffer (2 μl D-luciferin/ml MQ [L1349, Duchefa Biochemie]; 0.02% SILWET L-77 [Kurt Obermeier GmbH & Co. KG; Bad Berleburg, Germany]). After 2 to 4 h in the dark, the chemiluminescence signal was detected using a charge-coupled device imaging system CCD camera (0302110003, Princeton Instruments). Data acquisition was performed using the MetaVue program. Chemiluminescence was detected without any filters during a 5-min exposure. Raw pictures were analyzed and processed with ImageJ (https://imagej.nih.gov/ij). The mean (integrated density/area size) with extraction of the leaf background signal was used for the statistical evaluation of the data. Normalization was performed based on the total signal of all samples.

Co-IP

Co-IP was performed at Profacgen (https://www.profacgen.com). Briefly, constructs of interest were expressed in *N. tabacum* for 2 days, and subsequently, 3 g of tissue, ground in liquid nitrogen, was taken up in lysis buffer with protease inhibitors. The supernatant was collected by centrifugation. Washed empty Protein A/G beads were added to the supernatant for cleaning for 30 min and discarded. GFP antibody was added to the supernatant for 3 h. The Protein A/G beads were added again to fully bind the antibody for 2 h. Proteins were separated by SDS-PAGE, transferred to a membrane, and incubated with primary antibodies (anti-MYC and anti-GFP, 1:5,000), followed by secondary antibodies (anti-mouse/anti-rabbit [HRP, 1:5,000]), and developed (ECL).

Phloem exudate collection

Circa 4-week-old *S. lycopersicum* plants (Moneymaker) were placed in a large cage and exposed to a mixture of adult male and female whiteflies. Each week, a new batch of whiteflies was added to the cage to increase variation in nymphal stages. As a negative control, noninfested *S. lycopersicum* plants kept under similar conditions were used. After circa 4 weeks, phloem extraction was performed on well-infested plant leaves. Phloem exudate from tomato was extracted as described previously by Narvaez-Vasquez et al. (1994) and Madey et al. (2002), with slight modifications. Briefly, four leaves from each tomato plant were excised at the petiole and immersed in bleeding buffer (5 mM phosphate buffer, 5 mM EDTA) for 20 min. The petioles were trimmed in a Petri dish, for about 2 mm, while immersed in bleeding buffer, and transferred to an Eppendorf tube with 2 ml of phloem collection buffer (5 mM phosphate buffer, 5mM EDTA, and 0.5× protease inhibitor [Roche cOmplete EDTA-free Protease inhibitor]) and incubated for 6 h in humid conditions. Proteins in the exudates were concentrated by acetone precipitation (Mitton et al. 2009) and resuspended in Ambic buffer (100 mM ammonium bicarbonate, 10 mM tris(2-carboxyethyl)phosphine, 40 mM chloroacetamide). Trypsin digestion was carried out, and the next day, 1% formic acid was added to acidify the protein sample. For cleanup, an Omix C18 tip (Agilent, https://www.agilent.com/) was used, and the sample was eluted using elution buffer (60% acetonitrile, 0.1% formic acid, and 39.9% water). Five microliters sample was used for an LC-MS analysis as described in Tu et al. (2021). Raw MS/MS data were searched in Maxquant (version 1.6.14.0) (Cox and Mann 2008) against an in house-created *B. tabaci* proteome database and a *S. lycopersicum* database downloaded from Uniprot (in June 2020). To control for the false spectrum assignment rate (1% FDR), a reverse version of the same databases was also searched. Settings were set as default for timsDDA. Trypsin/P was selected as the digestion enzyme, with a maximum of two missed cleavages. The oxidation (M) was set as a variable modification and oarbamidomethyl (C) as a fixed modification. For accurate mass, retention, and TIMS-time matching: "match between runs" was selected with a matching time window of 0.2 min and a matching ion mobility window of 0.05 indices. The peptides are deposited to MassIVE with the dataset identifier PXD046758.

VIGS

Agroinfiltration. *Agrobacterium* carrying the TRV2 plasmid with a partial nucleotide sequence of the plant gene, the GFP or PDS (Liu et al. 2002), or the TRV1 plasmid were grown overnight at 28°C in LB medium supplemented with the appropriate antibiotics. The next day, the culture was diluted and grown overnight in LB supplemented with the appropriate antibiotics, 10 mM MES, and 20 μM acetosyringone. The bacterial pellet was resuspended in infiltration buffer and mixed with TRV1 to a final OD_{600} of 0.25 for each TRV2 construct. Cotyledons of 8- to 9-day-old *S. lycopersicum* plants (Moneymaker) were completely infiltrated with the *Agrobacterium* mixtures. After infiltration, the plants were watered and grown until use for the whitefly bioassays 4 to 5 weeks postinfiltration.

Analysis of *MIPDB141* expression. To visualize the silencing effect, a batch of plants was infiltrated with a construct silencing the *PDS* gene. This resulted in photobleaching, and the leaves turned white (Liu et al. 2002). For the *MIPDB141*- and *GFP*-VIGS plants, identically positioned leaves were taken and snap frozen in liquid nitrogen. Leaves of two to three separate plants were pooled as biological replicates (three for each batch). Harvested samples were ground to fine powder in liquid nitrogen with a mortar and pestle and stored at –80°C. Total RNA was extracted using the TRIzol/chloroform method. Purified RNA samples were DNase treated using TURBO DNAse (Invitrogen) to remove genomic DNA contamination according to the manufacturer's protocol. cDNA was synthesized from 1 μg of total RNA using the RevertAid H Minus Reverse Transcriptase (Thermo Scientific). Quantitative real-time PCR (ABI 7500 Real-Time PCR System, Applied Biosystems; https://www.thermofisher.com) was done using HOT FIREPol EvaGreen qPCR Mix Plus (ROX) (Solis BioDyne, Estonia). Two sets of primers were used to determine the mRNA levels in the leaf tissue: MIPset2 and TCTPset1 (see Supplementary Table S5). Products obtained by these primers were sequenced to confirm specificity for either *MIPDB141* or TCTP cDNA. A fourfold dilution series of cDNA was used to calculate primer efficiencies. Relative expression levels of *TCTP* and *MIPDB141* were calculated using the PfaffI analysis method in which the Ct values of *TCTP* and *MIPDB141* were normalized to the reference gene, *Actin* (see Supplementary Table S5).

VIGS combined with whitefly bioassay. Similar to the leaves selected for expression analysis, leaves for the bioassay were selected based on the photobleached phenotype related to *PDS* silencing. The leaf was used to cut a 24-mm disk, including a small part of the petiole. Then, the leaf disk was placed in a Petri dish as described in the section "Whitefly Bioassays." Plates were placed in a growth chamber at 25°C, 70% relative humidity, and a 16/8-h light/dark regime. The next day, 10 whitefly females were placed in each Petri dish, and Petri dishes were sealed again with Leukopore tape. The plates were incubated in a growth chamber for 2 days at 27°C under a 16/8-h light/dark regime. As a control, a gene involved in chloroplast development, not related to this study, was included to monitor the silencing effect (presence of light green spots) in leaf disks under these conditions (Supplementary Fig. S6D). After the incubation time, the plates were placed in a freezer at –20°C. Healthy-looking females (as described in the section "Whitefly Bioassays") were considered to be alive during freezing and counted as living females.

VIGS combined with choice assay. Whitefly choice assays were performed on square Petri dishes (120 mm × 120 mm) whereby 0.6% plant agar was poured to the edge (while keeping the plates at a 45° angle). After drying on the opposite side, the same was done. The agar was then covered with transparent foil (Supplementary Fig. S6B). Small cuts in the foil were made to be able to place the disks in the agar, as described before. Three disks of the same *MIPDB141*-silenced plant were placed on one side, three disks of the *GFP*-silenced plant were placed on the other side, and 15 whiteflies in chill coma were placed in the middle of the plate. The plates were then sealed with Leukopore tape and placed in random orientation in the growth cabinet under the same conditions as described in the section "VIGS Combined with Whitefly Bioassay." After 2 days, the plates were carefully transported to a freezer at –20°C. Scoring was performed by analyzing the position

of the whiteflies (GFP or MIPDB141 site). The number of eggs produced was divided by the number of females found on the corresponding site. The choice assay was performed twice, with either 6 or 8 plates containing 15 whiteflies per plate.

Statistical analyses. Statistical analyses for ROS assays were performed by taking the average of the two disks from the same infiltration spot or disks. Total luminance of eight plants was used for further statistical analysis. The data were analyzed for normality with SPSS and were either used in a Student's *t*-test or Mann-Whitney *U*-test. In case of more than two different effector constructs, either repeated-measures analysis of variance (ANOVA) or Friedman test was used. Values of $P \leq 0.05$ were considered significantly different compared with the CFP control group. Statistical analysis for the bioassays was performed on the eggs produced per living female using an approach similar to the ROS assay. For VIGS, a factorial ANOVA was used. Statistical analysis on the VIGS choice test was performed using a replicated *G*-test for goodness of fit. For the luciferase complementation assay, normalized data of eight plants were used for repeated-measures ANOVA tests in SPSS. Statistical analysis on the expression levels in the VIGS assay was performed using R (R Core Team (2022). A Shapiro-Wilk test was applied for analyzing the normal distribution of values. For comparison of the relative expression between *GFP*- and *MIPDB141*/*TCTP*-silenced plants, Mann-Whitney *U*-tests were performed.

Acknowledgments

The authors thank the Van Leeuwenhoek Center for Advanced Microscopy (LCAM; University of Amsterdam) for use of microscopes, Rodrigo Therezan de Freitas for guidance in the VIGS assay, Harold Lemereis and Ludek Tikovsky for the excellent plant care, and Eva van Doore for technical support.

Literature Cited

Abd-El-Haliem, A. M., Hoogstrate, S. W., and Schuurink, R. C. 2018. A robust functional genomics approach to identify effector genes required for thrips (*Frankliniella occidentalis*) reproductive performance on tomato leaf disks. Front. Plant Sci. 9:1852.

Aoki, K., Suzui, N., Fujimaki, S., Dohmae, N., Yonekura-Sakakibara, K., Fujiwara, T., Hayashi, H., Yamaya, T., and Sakakibara, H. 2005. Destination-selective long-distance movement of phloem proteins. Plant Cell 17:1801-1814.

Berkowitz, O., Jost, R., Pollmann, S., and Masle, J. 2008. Characterization of TCTP, the translationally controlled tumor protein, from *Arabidopsis thaliana*. Plant Cell 20:3430-3447.

Bird, D. M., and Wilson, M. A. 1994. DNA sequence and expression analysis of root-knot nematode-elicited giant cell transcripts. Mol. Plant-Microbe Interact. 7:419-24.

Bisht, D. S., Bhatia, V., and Bhattacharya, R. 2019. Improving plant-resistance to insect-pests and pathogens: The new opportunities through targeted genome editing. Semin. Cell Dev. Biol. 96:65-76.

Bommer, U.-A., and Thiele, B.-J. 2004. The translationally controlled tumour protein (TCTP). Int. J. Biochem. Cell Biol. 36:379-385.

Boykin, L. M., Bell, C. D., Evans, G., Small, I., and De Barro, P. J. 2013. Is agriculture driving the diversification of the *Bemisia tabaci* species complex (Hemiptera: Sternorrhyncha: Aleyrodidae)? Dating, diversification and biogeographic evidence revealed. BMC Evol. Biol. 13:228.

Chen, W., Hasegawa, D. K., Kaur, N., Kliot, A., Pinheiro, P. V., Luan, J., Stensmyr, M. C., Zheng, Y., Liu, W., Sun, H., Xu, Y., Luo, Y., Kruse, A., Yang, X., Kontsedalov, S., Lebedev, G., Fisher, T. W., Nelson, D. R., Hunter, W. B., Brown, J. K., Jander, G., Cilia, M., Douglas, A. E., Ghanim, M., Simmons, A. M., Wintermantel, W. M., Ling, K.-S., and Fei, Z. 2016. The draft genome of whitefly *Bemisia tabaci* MEAM1, a global crop pest, provides novel insights into virus transmission, host adaptation, and insecticide resistance. BMC Biol. 14:110.

Cox, J., and Mann, M. 2008. MaxQuant enables high peptide identification rates, individualized p.p.b.-range mass accuracies and proteome-wide protein quantification. Nat. Biotechnol. 26:1367-1372.

Craig, R., and Beavis, R. C. 2004. TANDEM: Matching proteins with tandem mass spectra. Bioinformatics 20:1466-1467.

De Barro, P. J., Liu, S.-S., Boykin, L. M., and Dinsdale, A. B. 2011. *Bemisia tabaci*: A statement of species status. Annu. Rev. Entomol. 56:1-19.

Deng, Z., Chen, J., Leclercq, J., Zhou, Z., Liu, C., Liu, H., Yang, H., Montoro, P., Xia, Z., and Li, D. 2016. Expression profiles, characterization and function of *HbTCTP* in rubber tree (*Hevea brasiliensis*). Front. Plant Sci. 7:789.

Du, H., Xu, H.-X., Wang, F., Qian, L.-X., Liu, S.-S., and Wang, X.-W. 2022. Armet from whitefly saliva acts as an effector to suppress plant defences by targeting tobacco cystatin. New Phytol. 234:1848-1862.

Felix, G., Duran, J. D., Volko, S., and Boller, T. 1999. Plants have a sensitive perception system for the most conserved domain of bacterial flagellin. Plant J. 18:265-276.

Fernandez-Pozo, N., Menda, N., Edwards, J. D., Saha, S., Tecle, I. Y., Strickler, S. R., Bombarely, A., Fisher-York, T., Pujar, A., Foerster, H., Yan, A., and Mueller, L. A. 2015. The Sol Genomics Network (SGN)—from genotype to phenotype to breeding. Nucleic Acids Res. 43: D1036-D1041.

Fiallo-Olivé, E., Pan, L.-L., Liu, S.-S., and Navas-Castillo, J. 2020. Transmission of begomoviruses and other whitefly-borne viruses: Dependence on the vector species. Phytopathology 110:10-17.

Firdaus, S., Van Heusden, A., Harpenas, A., Supena, E. D. J., Visser, R. G. F., and Vosman, B. 2011. Identification of silverleaf whitefly resistance in pepper. Plant Breed. 130:708-714.

Formstecher, E., Aresta, S., Collura, V., Hamburger, A., Meil, A., Trehin, A., Reverdy, C., Betin, V., Maire, S., Brun, C., Jacq, B., Arpin, M., Bellaiche, Y., Bellusci, S., Benaroch, P., Bornens, M., Chanet, R., Chavrier, P., Delattre, O., Doye, V., Fehon, R., Faye, G., Galli, T., Girault, J.-A., Goud, B., de Gunzburg, J., Johannes, L., Junier, M.-P., Mirouse, V., Mukherjee, A., Papadopoulo, D., Perez, F., Plessis, A., Rossé, C., Saule, S., Stoppa-Lyonnet, D., Vincent, A., White, M., Legrain, P., Wojcik, J., Camonis, J., and Daviet, L. 2005. Protein interaction mapping: A *Drosophila* case study. Genome Res. 15:376-384.

Gangwar, R. K., and Gangwar, C. 2018. Lifecycle, distribution, nature of damage and economic importance of whitefly, *Bemisia tabaci* (Gennadius). Acta Sci. Agric. 2.4:36-39.

Geer, L. Y., Markey, S. P., Kowalak, J. A., Wagner, L., Xu, M., Maynard, D. M., Yang, X., Shi, W., and Bryant, S. H. 2004. Open mass spectrometry search algorithm. J. Proteome Res. 3:958-964.

Goggin, F. L., and Fischer, H. D. 2021. Reactive oxygen species in plant interactions with aphids. Front. Plant Sci. 12:811105.

Gutiérrez-Galeano, D. F., Toscano-Morales, R., Calderón-Pérez, B., Xoconostle- Cázares, B., and Ruiz-Medrano, R. 2014. Structural divergence of plant TCTPs. Front. Plant Sci. 5:361.

Hall, T. A. 1999. BioEdit: A user-friendly biological sequence alignment editor and analysis program for Windows 95/98/NT. Nucleic. Acids. Symp. Ser. 41:95-98.

Hoepflinger, M. C., Reitsamer, J., Geretschlaeger, A. M., Mehlmer, N., and Tenhaken, R. 2013. The effect of translationally controlled tumour protein (TCTP) on programmed cell death in plants. BMC Plant Biol. 13: 135.

Holsters, M., de Waele, D., Depicker, A., Messens, E., van Montagu, M., and Schell, J. 1978. Transfection and transformation of *Agrobacterium tumefaciens*. Mol. Gen. Genet. 163:181-187.

Horowitz, A. R., Ghanim, M., Roditakis, E., Nauen, R., and Ishaaya, I. 2020. Insecticide resistance and its management in *Bemisia tabaci* species. J. Pest. Sci. 93:893-910.

Huang, H.-J., Ye, Z.-X., Lu, G., Zhang, C.-X., Chen, J.-P., and Li, J.-M. 2021. Identification of salivary proteins in the whitefly *Bemisia tabaci* by transcriptomic and LC–MS/MS analyses. Insect Sci. 28:1369-1381.

Jay, F., Brioudes, F., and Voinnet, O. 2023. A contemporary reassessment of the enhanced transient expression system based on the tombusviral silencing suppressor protein P19. Plant J. 113:186-204.

Jiang, Y., Zhang, C.-X., Chen, R., and He, S. Y. 2019. Challenging battles of plants with phloem-feeding insects and prokaryotic pathogens. Proc. Natl. Acad. Sci. U.S.A. 116:23390-23397.

Jonckheere, W., Dermauw, W., Zhurov, V., Wybouw, N., Van den Bulcke, J., Villarroel, C. A., Greenhalgh, R., Grbić, M., Schuurink, R. C., Tirry, L., Baggerman, G., Clark, R. M., Kant, M. R., Vanholme, B., Menschaert, G., and Van Leeuwen, T. 2016. The salivary protein repertoire of the polyphagous spider mite *Tetranychus urticae*: A quest for effectors. Mol. Cell. Proteomics 15:3594-3613.

Kempema, L. A., Cui, X., Holzer, F. M., and Walling, L. L. 2007. Arabidopsis transcriptome changes in response to phloem-feeding silverleaf whitefly nymphs: Similarities and distinctions in responses to aphids. Plant Physiol. 143:849-865.

Keppler, L. D., Baker, C. J., and Atkinson, M. M. 1989. Active oxygen production during a bacteria-induced hypersensitive reaction in tobacco suspension cells. Phytopathology 79:974-978.

Kerchev, P. I., Fenton, B., Foyer, C. H., and Hancock, R. D. 2012. Plant responses to insect herbivory: Interactions between photosynthesis, reactive oxygen species and hormonal signalling pathways. Plant Cell Environ. 35:441-453.

Kim, S., and Pevzner, P. A. 2014. MS-GF+ makes progress towards a universal database search tool for proteomics. Nat. Commun. 5:5277.

Ko, J.-H., Chow, K.-S., and Han, K.-H. 2003. Transcriptome analysis reveals novel features of the molecular events occurring in the laticifers of *Hevea brasiliensis* (para rubber tree). Plant Mol. Biol. 53:479-492.

Lee, H.-R., Lee, S., Park, S., van Kleeff, P. J. M., Schuurink, R. C., and Ryu, C.-M. 2018. Transient expression of whitefly effectors in *Nicotiana benthamiana* leaves activates systemic immunity against the leaf pathogen *Pseudomonas syringae* and soil-borne pathogen *Ralstonia solanacearum*. Front. Ecol. Evol. 6:90.

Li, D., Li, H.-Y., Zhang, J.-R., Wu, Y.-J., Zhao, S.-X., Liu, S.-S., and Pan, L.-L. 2023. Plant resistance against whitefly and its engineering. Front. Plant Sci. 14:1232735.

Liu, T.-X., Stansly, P. A., and Gerling, D. 2015. Whitefly parasitoids: Distribution, life history, bionomics, and utilization. Annu. Rev. Entomol. 60:273-292.

Liu, Y., Schiff, M., and Dinesh-Kumar, S. P. 2002. Virus-induced gene silencing in tomato. Plant J. 31:777-786.

Madey, E., Nowack, L. M., and Thompson, J. E. 2002. Isolation and characterization of lipid in phloem sap of canola. Planta 214:625-634.

Maio, F. 2019. Shedding light on the multiple functions of the geminivirus replication initiator protein. Doctoral dissertation. University of Amsterdam, Amsterdam.

Martens, L., Hermjakob, H., Jones, P., Adamski, M., Taylor, C., States, D., Gevaert, K., Vandekerckhove, J., and Apweiler, R. 2005. PRIDE: The proteomics identifications database. Proteomics 5:3537-3545.

Mitton, F. M., Pinedo, M. L., and de la Canal, L. 2009. Phloem sap of tomato plants contains a DIR1 putative ortholog. J. Plant Physiol. 166:543-547.

Mugerwa, H., Seal, S., Wang, H.-L., Patel, M. V., Kabaalu, R., Omongo, C. A., Alicai, T., Tairo, F., Ndunguru, J., Sseruwagi, P., and Colvin, J. 2018. African ancestry of New World, *Bemisia tabaci*-whitefly species. Sci. Rep. 8:2734.

Mugerwa, H., Wang, H.-L., Sseruwagi, P., Seal, S., and Colvin, J. 2021. Whole-genome single nucleotide polymorphism and mating compatibility studies reveal the presence of distinct species in sub-Saharan Africa *Bemisia tabaci* whiteflies. Insect Sci. 28:1553-1566.

Naalden, D., van Kleeff, P. J. M., Dangol, S., Mastop, M., Corkill, R., Hogenhout, S. A., Kant, M. R., and Schuurink, R. C. 2021. Spotlight on the roles of whitefly effectors in insect–plant interactions. Front. Plant Sci. 12:661141.

Nakagawa, T., Kurose, T., Hino, T., Tanaka, K., Kawamukai, M., Niwa, Y., Toyooka, K., Matsuoka, K., Jinbo, T., and Kimura, T. 2007. Development of series of gateway binary vectors, pGWBs, for realizing efficient construction of fusion genes for plant transformation. J. Biosci. Bioeng. 104:34-41.

Nakamura, S., Mano, S., Tanaka, Y., Ohnishi, M., Nakamori, C., Araki, M., Niwa, T., Nishimura, M., Kaminaka, H., Nakagawa, T., Sato, Y., and Ishiguro, S. 2010. Gateway binary vectors with the bialaphos resistance gene, *bar*, as a selection marker for plant transformation. Biosci. Biotechnol. Biochem. 74:1315-1319.

Narvaez-Vasquez, J., Orozco-Cardenas, M. L., and Ryan, C. A. 1994. A sulfhydryl reagent modulates systemic signaling for wound-induced and systemin-induced proteinase inhibitor synthesis. Plant Physiol. 105: 725-730.

Nombela, G., Williamson, V. M., and Muñiz, M. 2003. The root-knot nematode resistance gene *Mi-1.2* of tomato is responsible for resistance against the whitefly *Bemisia tabaci*. Mol. Plant-Microbe Interact. 16:645-649.

Pant, S., and Huang, Y. 2021. Elevated production of reactive oxygen species is related to host plant resistance to sugarcane aphid in sorghum. Plant Signal. Behav. 16:1849523.

Patra, B., and Kumar Hath, T. 2022. Insecticide resistance in whiteflies *Bemisia tabaci* (Gennadius): Current global status. In: Insecticides – Impact and Benefits of Its Use for Humanity. R. E. R. Ranz, ed. IntechOpen, London.

Paulmurugan, R., and Gambhir, S. S. 2007. Combinatorial library screening for developing an improved split-firefly luciferase fragment-assisted complementation system for studying protein−protein interactions. Anal. Chem. 79:2346-2353.

Paysan-Lafosse, T., Blum, M., Chuguransky, S., Grego, T., Pinto, B. L., Salazar, G. A., Bileschi, M. L., Bork, P., Bridge, A., Colwell, L., Gough, J., Haft, D. H., Letunić, I., Marchler-Bauer, A., Mi, H., Natale, D. A., Orengo, C. A., Pandurangan, A. P., Rivoire, C., Sigrist, C. J. A., Sillitoe, I., Thanki, N., Thomas, P. D., Tosatto, S. C. E., Wu, C. H., and Bateman, A. 2023. InterPro in 2022. Nucleic Acids Res. 51:D418-D427.

Peng, Z., Su, Q., Ren, J., Tian, L., Zeng, Y., Yang, Y., Wang, S., Xie, W., Wu, Q., Li, Z., and Zhang, Y. 2023. A novel salivary effector, BtE3, is essential for whitefly performance on host plants. J. Exp. Bot. 74: 2146-2159.

Pennington, H. G., Gheorghe, D. M., Damerum, A., Pliego, C., Spanu, P. D., Cramer, R., and Bindschedler, L. V. 2016. Interactions between the powdery mildew effector BEC1054 and barley proteins identify candidate host targets. J. Proteome Res. 15:826-839.

R Core Team 2022. R: A Language and Environment for Statistical Computing. R Foundation for Statistical Computing, Vienna. https://www.R-project.org

Sani, I., Ismail, S. I., Abdullah, S., Jalinas, J., Jamian, S., and Saad, N. 2020. A review of the biology and control of whitefly, *Bemisia tabaci* (Hemiptera: Aleyrodidae), with special reference to biological control using entomopathogenic fungi. Insects 11:619.

Saurabh, S., Mishra, M., Rai, P., Pandey, R., Singh, J., Khare, A., Jain, M., and Singh, P. K. 2021. Tiny flies: A mighty pest that threatens agricultural productivity—A case for next-generation control strategies of whiteflies. Insects 12:585.

Shi, J., Zhu, Y., Li, M., Ma, Y., Liu, H., Zhang, P., Fang, D., Guo, Y., Xu, P., and Qiao, Y. 2020. Establishment of a novel virus-induced virulence effector assay for the identification of virulence effectors of plant pathogens using a PVX-based expression vector. Mol. Plant Pathol. 21: 1654-1661.

Snoeck, S., Guayazán-Palacios, N., and Steinbrenner, A. D. 2022. Molecular tug-of-war: Plant immune recognition of herbivory. Plant Cell 34:1497-1513.

Sperschneider, J., Catanzariti, A.-M., DeBoer, K., Petre, B., Gardiner, D. M., Singh, K. B., Dodds, P. N., and Taylor, J. M. 2017. LOCALIZER: Subcellular localization prediction of both plant and effector proteins in the plant cell. Sci. Rep. 7:44598.

Struk, S., Jacobs, A., Sánchez Martín-Fontecha, E., Gevaert, K., Cubas, P., and Goormachtig, S. 2019. Exploring the protein–protein interaction landscape in plants. Plant Cell Environ. 42:387-409.

Su, Q., Peng, Z., Tong, H., Xie, W., Wang, S., Wu, Q., Zhang, J., Li, C., and Zhang, Y. 2019. A salivary ferritin in the whitefly suppresses plant defenses and facilitates host exploitation. J. Exp. Bot. 70:3343-3355.

Teufel, F., Almagro Armenteros, J. J., Johansen, A. R., Gíslason, M. H., Pihl, S. I., Tsirigos, K. D., Winther, O., Brunak, S., von Heijne, G., and Nielsen, H. 2022. SignalP 6.0 predicts all five types of signal peptides using protein language models. Nat. Biotechnol. 40:1023-1025.

Tu, Z., Dekker, H. L., Roseboom, W., Swarge, B. N., Setlow, P., Brul, S., and Kramer, G. 2021. High resolution analysis of proteome dynamics during *Bacillus subtilis* sporulation. Int. J. Mol. Sci. 22:9345.

Tyagi, S., Kesiraju, K., Saakre, M., Rathinam, M., Raman, V., Pattanayak, D., and Sreevathsa, R. 2020. Genome editing for resistance to insect pests: An emerging tool for crop improvement. ACS Omega 5:20674-20683.

van Kleeff, P. J. M., Mastop, M., Sun, P., Dangol, S., van Doore, E., Dekker, H. L., Kramer, G., Lee, S., Ryu, C.-M., de Vos, M., and Schuurink, R. 2023. Discovery of three *Bemisia tabaci* effectors and their effect on gene expression in planta. Mol. Plant-Microbe Interact. https://doi.org/10.1094/MPMI-04-23-0044-R

Vaudel, M., Barsnes, H., Berven, F. S., Sickmann, A., and Martens, L. 2011. SearchGUI: An open-source graphical user interface for simultaneous OMSSA and X!Tandem searches. Proteomics 11:996-999.

Vaudel, M., Burkhart, J. M., Zahedi, R. P., Oveland, E., Berven, F. S., Sickmann, A., Martens, L., and Barsnes, H. 2015. PeptideShaker enables reanalysis of MS-derived proteomics data sets. Nat. Biotechnol. 33:22-24.

Vizcaíno, J. A., Deutsch, E. W., Wang, R., Csordas, A., Reisinger, F., Ríos, D., Dianes, J. A., Sun, Z., Farrah, T., Bandeira, N., Binz, P.-A., Xenarios, I., Eisenacher, M., Mayer, G., Gatto, L., Campos, A., Chalkley, R. J., Kraus, H.-J., Albar, J. P., Martinez-Bartolomé, S., Apweiler, R., Omenn, G. S., Martens, L., Jones, A. R., and Hermjakob, H. 2014. ProteomeXchange provides globally coordinated proteomics data submission and dissemination. Nat. Biotechnol. 32:223-226.

Vleeshouwers, V. G. A. A., and Oliver, R. P. 2014. Effectors as tools in disease resistance breeding against biotrophic, hemibiotrophic, and necrotrophic plant pathogens. Mol. Plant-Microbe Interact. 27:196-206.

Wang, N., Zhao, P., Ma, Y., Yao, X., Sun, Y., Huang, X., Jin, J., Zhang, Y., Zhu, C., Fang, R., and Ye, J. 2019. A whitefly effector Bsp9 targets host immunity regulator WRKY33 to promote performance. Phil. Trans. R. Soc. B 374:20180313.

Wang, R., and Brattain, M. G. 2007. The maximal size of protein to diffuse through the nuclear pore is larger than 60 kDa. FEBS Lett. 581:3164-3170.

Wang, S., Guo, H., Ge, F., and Sun, Y. 2020. Apoptotic neurodegeneration in whitefly promotes the spread of TYLCV. eLife 9:e56168.

Wang, Y., Akiyama, H., Terakado, K., and Nakatsu, T. 2013. Impact of site-directed mutant luciferase on quantitative green and orange/red emission intensities in firefly bioluminescence. Sci. Rep. 3:2490.

Xu, H.-X., Qian, L.-X., Wang, X.-W., Shao, R.-X., Hong, Y., Liu, S.-S., and Wang, X.-W. 2019. A salivary effector enables whitefly to feed on host plants by eliciting salicylic acid-signaling pathway. Proc. Natl. Acad. Sci. U.S.A. 116:490-495.

Yang, C.-H., Guo, J.-Y., Chu, D., Ding, T.-B., Wei, K.-K., Cheng, D.-F., and Wan, F.-H. 2017. Secretory laccase 1 in *Bemisia tabaci* MED is involved in whitefly-plant interaction. Sci. Rep. 7:3623.